

Unlimited Sampling for FMCW Radars: A Proof of Concept

**Thomas Feuillen, Mohammad Alae-Kerahroodi,
Bhavani Shankar M. R., and Bjorn Ottersten***

University of Luxembourg
LUXEMBOURG

Thomas.feuillen@uni.lu

Ayush Bhandari
Imperial College
UNITED KINGDOM

ABSTRACT

High-resolution FMCW radar systems are becoming an integral aspect of applications ranging from automotive safety and autonomous driving to health monitoring of infants and the elderly. This integration provides challenging scenarios that require radars with extremely high dynamic range (HDR) ADCs; these ADCs need to avoid saturation while offering high-performance and high-fidelity data-acquisition. The recent concept of Unlimited Sensing allows one to achieve high dynamic range (HDR) acquisition by recording low dynamic range, modulo samples. Interestingly, oversampling of these folded measurements, with a sampling rate independent of the modulo threshold, is sufficient to guarantee their perfect reconstruction for band-limited signals. This contrasts with the traditional methodology of increasing the dynamic range by adding a programmable-gain amplifier or operating multiple ADCs in parallel. This paper demonstrates an FMCW radar prototype that utilises the unlimited sampling strategy. Our hardware experiments show that even with the use of a modulo measurements of lower precision, the US reconstruction is able to match the performances of the conventional acquisition. Furthermore, our real-time processing capability demonstrates that our “proof-of-concept” approach is a viable solution for HDR FMCW radar signal processing, thus opening a pathway for future hardware-software optimization and integration of this technology with other mainstream systems.

1.0 INTRODUCTION

Developing high dynamic range (HDR) Analog-to-digital converter (ADC) is pivotal to radar technology. Factors such as the inverse-square law and material reflectivity impose physical constraints on the dynamic range (DR) in ranging applications and this is also the case with radar systems. Due to the inverse-square, amplitude decay is natural as the distance of the object increases from the radar. This, in part, results in the common-place problem of detecting weak targets in strong background target or clutter response. Other scenarios where the DR leads to measurement challenges include,

- 1) Detecting humans (e.g. children) next to large objects e.g. truck, or a strong clutter [1].
- 2) Recording radar reflectivity measurements from moderate to heavy precipitation in weather radar [2].
- 3) Obtaining maximum possible penetration depth in strongly inhomogeneous materials in Ground Penetrating Radar (GPR) [3].

Current Approaches to the DR Problem. The different solutions for addressing the DR issue in radar systems include,

- One-time calibration of the ADC to match the DR of the signal of interest.

- Using Automatic Gain Control (AGC) prior to the ADC to automate the above solution.
- Using multiple ADCs with different gains, namely, *interleaved gain* ADC [5], [6].

In the last approach, the idea is to attenuate a selective subset of the data before it gets sampled, so that if clipping is detected after the sampling process, it is possible to estimate the missing samples using the non-clipped samples that were attenuated. But the increment in signal distortion and its noise level are side effects of these approaches. This is similar to HDR photography and imaging [7], [8].

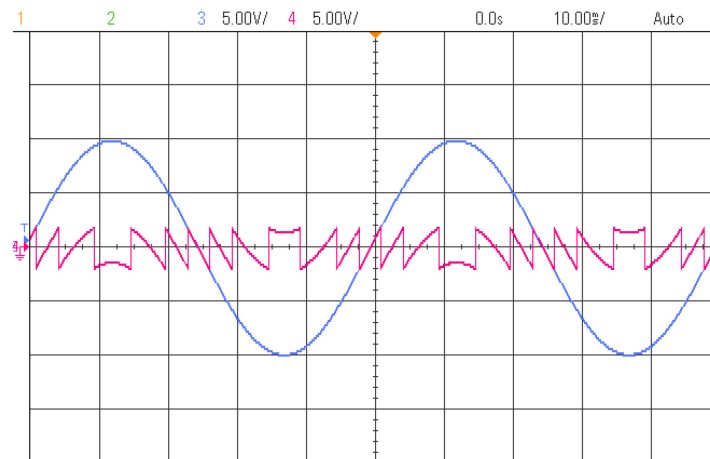


Figure 1: An oscilloscope snapshot of the operation of unlimited sampling ADCs [4].

FMCW Radars at Lower Sampling Rates. Frequency Modulated Continuous Wave (FMCW) radar sensors are known to be a cheap and efficient solution for sensing in automotive and indoor applications. By resorting to analog domain dechirping operations, also referred to as *stretch processing*¹, the FMCW radars register a narrowband signal at the receiver. The key advantage of de-chirping is that the received signal can be sampled at much smaller sampling rates compared to the signal's bandwidth [10]–[12]. Not surprisingly, this advantage has been capitalized in different application scenarios and research efforts have been focused towards enhancing DR of the radar systems [11], [13], [14]. For instance, the approach in [14] utilizes a phase noise based detection procedure to improve the DR of an airborne FMCW cloud radar (operating in 167 GHz frequency) by 18dB. However, this entails a cost in that one has to pay a detection sensitivity penalty of about 3dB, which can be non-negligible in certain applications.

In FMCW radar based applications, large dynamic range of the sensor leads to the possibility of measuring of widely varying amplitudes without attenuating the strong reflections by using an AGC. However, adding these AGCs results in a increase in price and size of the device; a bottleneck in mass production.

Our Approach: Modulo Sensing for Radars. Conventional digital acquisition pipelines consider hardware and algorithms independently. Thus any loss of information during acquisition has implications when utilizing recovery algorithms. To overcome the fundamental DR issue in digital acquisition, an alternative sampling pipeline has been proposed recently, namely, Unlimited Sampling Framework (USF) [4], [15]–[17]. The USF leverages a joint design of hardware and algorithms to overcome the clipping or saturation problem. In particular,

¹ This involves transmitting a wideband FMCW signal and mixing the reflected echoes with an accurately timed local oscillator of the same chirp-rate [9].

- On the **hardware front**, modulo non-linearity is injected so that the continuous time signal is folded into the dynamic range of the ADC. Thereon, one samples the low dynamic range (LDR) signal using the unlimited sampling ADCs, hereafter referred to as US-ADCs. For a hardware validation of the USF approach we refer to [4]. An exemplary output of the US-ADC is shown in Figure 1².
- On the **algorithmic front**, mathematically guaranteed reconstruction methods are utilized for reconstructing the HDR signal from its LDR, modulo samples. For instance, in [15], [17], a *Shannon-Nyquist* like sampling theorem was proven that showed that modulo samples can be recovered from a constant factor oversampling (cf. Theorem 1). Non-linear reconstruction strategies that can handle hardware data in presence of noise and non-idealities have been presented in [4].

Motivation and Contributions. Through the examples different examples in our discussion and literature, we have seen that the wide spread dynamic range problem in the context of radars naturally necessitates solutions for HDR signal acquisition. To this end, we take a first step towards a “modulo sampling” based radar. Our key observation is that owing to the de-chirping process, the received signal in FMCW radars is narrowband and this matches the hypothesis of the USF. At the same time, the new signal models, hardware pipeline and use of modulo non-linearities requires non-trivial tailoring of both hardware and algorithms alike. In this context, and to the best of the author’s knowledge, this is the first application of the USF to practical noisy radar data that is, moreover, performed on a real-time platform. This first iteration of the USF-FMCW radar, showcases that high-dynamic range FMCW radar signals can be successfully acquired and perfectly reconstructed from their modulo measurements, allowing for the recovery of weaker targets. This work paves the way to new and more efficient radar architectures with a joint acquisition-reconstruction design approach using USF.

The structure of the paper is as follow: a short overview of the FMCW radar is provided in Section II, Section III introduces the USF, finally experimental results are presented in Section IV before concluding in Section V.

2.0 FMCW RADAR MODEL

This work aims to showcase the potentialities that the USF provides to radar signal processing and its impact on their associated hardware. To that end, we restrict our setting to a simple FMCW radar with one transmit and one receive antenna pair. This simple setting leads to a 1-D estimation problem, as this radar can only infer the range; yet, this alone enables us to clearly highlight the advantages that the USF provides to radar signal processing.

The radar transmits a signal $s(t)$ defined as:

$$s(t) = \sqrt{P} \cos \left(\int_0^t 2\pi f(t) + \phi \right),$$

where, $f(t)$ is the carrier frequency function defined as:

$$f(t) = f_0 + B \frac{t}{T_c},$$

where,

- f_0 the carrier frequency.
- B the bandwidth spanned by the chirp function $f(t)$.
- T_c the duration of the chirp.

² A live demonstration of this hardware is available at the following link <https://youtu.be/I9f1S0F3s5E>.

Let us consider a simple scenario with one target located at a range R in front of the radar. The received signal can be expressed, after dechirping as

$$r(t) = \alpha \cos\left(-2\pi f(t) \frac{2R}{c} + \phi\right) = \alpha \cos\left(-2\pi B \frac{t}{T} \frac{2R}{c} + \phi'\right), \quad (1)$$

where c is the speed of light and $\phi' = \phi + 2\pi f_0 \frac{2R}{c}$. In words, the coherent demodulation translates the time delay $2R/c$ into a frequency shift proportional to the range of the targets $B \frac{2R}{Tc}$.

Considering now a purely additive model, the signal back-scattered from a scene with K targets at different ranges R_k is simply a sum of sines with different frequencies related to their respective ranges,

$$r(t) = \sum_{k=1}^{k=K} \alpha_k \cos\left(-2\pi B \frac{t}{T} \frac{2R_k}{c} + \phi_k\right).$$

The power received from each targets, i.e. α_k , with $k \in [K]$, can vary by multiple order of magnitudes because of their range or Radar Cross Section (RCS). In a similar manner to Shannon's sampling theorem, the novel theory of unlimited sampling proves that a bandlimited function with a wide dynamic range can be precisely reconstructed from oversampled, low dynamic range samples [22]. In parallel to this fact, the performance efficiency of radar receivers is often greatly influenced by the power imbalance between multiple targets in the scene. Indeed, to be able to detect a weak target in the background of a strong target (clutter), a high dynamic range ADC is required. In this context, the received signal model in (1) can be sampled and reconstructed using the USF which provides a very high dynamic range.

3.0 UNLIMITED SAMPLING

This section reviews the acquisition model and reconstruction guarantees for the USF, specifically in the context of bandlimited signal classes. The key to the USF is that modulo non-linearity preceding the sampler or the ADC, precludes saturation [4], [15]–[17]. As demonstrated recently in [4], the modulo non-linearity can indeed be implemented in hardware and the reconstruction algorithms lead to the desired HDR signal recovery, up to 24λ [4], in practice. In this paper, we implement the USF concept using an actual radar and evaluate its performance with real time acquisition and processing. Our experimental platform acquires the radar signal with an ADC of finite resolution which introduces quantization noise. For the sake of conciseness however, this section only introduces the unlimited sampling framework in the context of unquantized acquisition. The effect of quantization in the context of unlimited sampling has been studied in [17].

3.1 Model and Theory

USF proposes to record folded versions of the signal. These measurements are expressed as

$$\mathcal{M}_\lambda(r(t)) \stackrel{\text{def}}{=} r(t) - 2\lambda \left\lfloor \frac{r(t)}{2\lambda} + \frac{1}{2} \right\rfloor, \quad \lambda \in \mathbb{R}^+ \quad (2)$$

where $\lfloor r \rfloor$ is the flooring function. The operator $\mathcal{M}_\lambda(\cdot)$ effectively folds the measurements around $\pm\lambda$ (see Figure 1).

While the US-ADC has an obvious advantage over traditional ADC architecture in that it circumvents the signal saturation problem, the full potential of this approach is only relevant if signal of interest can be reconstructed from these folded measurements. The aim of this paper is not to provide an exhaustive overview of the theory of Unlimited-Sampling (we refer the reader to [17]). We, nonetheless, provide hereafter the main result that motivate the use USF in FMCW radar signal processing.

Theorem 1 (Unlimited Sampling Theorem, [15]). *Let $g(t)$ be a finite energy, bandlimited signal with maximum frequency Ω and let $y[n]$, $n \in \mathbb{Z}$ in (2) be the modulo samples of $g(t)$ with sampling rate $1/T$. Then a sufficient condition for recovery of $g(t)$ from $y[n]$ is that $T \leq 1/2\Omega e$ (up to additive multiples of 2λ) where e denotes Euler's constant.*

The result of Theorem 1 is striking. Similar to Shannon's sampling theorem, introduced in [23]. Theorem 1 asserts that any band-limited signal can be successfully recovered from modulo measurements as long as the sampling rate is high enough. Interestingly, this rate is only a multiple of the one prescribed by Shannon, and does not depend on the dynamic range of the US-ADC, i.e., it does not depend on λ .

3.2 Reconstruction Algorithm

The key idea behind the recovery of a signal from its modulo samples is that the higher-order finite differences commute with the modulo operation in a certain sense. Under appropriate conditions (cf. Theorem 1) the higher order difference of the modulo samples matches the high order differences of the original measurements [17]. Let

$$s[k] \stackrel{\text{def}}{=} \mathcal{M}_\lambda(r(t))|_{t=kT}, \quad k \in \mathbb{Z},$$

denote the modulo samples of the Ω -bandlimited signal $r(t)$, at $t = kT$, where $T \leq 1/2\Omega e$ is the sampling time. The first order difference of a signal $s[k]$ is denoted by $(\Delta s)[k] = s[k+1] - s[k]$. Then, $(\Delta^N s)[k]$ is the N -th order difference can be obtained by recursive application of the finite-difference operator, $\Delta^N s = \Delta^{N-1}(\Delta s)$. For N given by,

$$N = \left\lceil \frac{\log \lambda - \log \hat{\beta}_g}{\log(T\Omega e)} \right\rceil,$$

With $\hat{\beta}_g \geq \max_t |r(t)|$ applying $\mathcal{M}_\lambda(\cdot)$ on $(\Delta^N s)[k]$, we obtain $(\Delta^N r)[k]$ or,

$$N = \left\lceil \frac{\log \lambda - \log \hat{\beta}_g}{\log(T\Omega e)} \right\rceil \Rightarrow (\Delta^N r)[k] = \mathcal{M}_\lambda(\Delta^N s)[k].$$

Thereon, it remains to invert $\Delta^N r$. Instead of inverting a bandlimited sequence, in the unlimited sampling algorithm, one inverts $\Delta^N \epsilon_r = \Delta^N(r - s) = \mathcal{M}_\lambda(\Delta^N s) - \Delta^N s$ because $\Delta^N \epsilon_r \in 2\mathbb{Z}$, $n \leq N$. Algorithm 1 recovers ϵ_r (up to an unknown constant) and thereon, $\epsilon_r[k] + s[k] \mapsto r[k]$.

Algorithm 1: Unlimited Sampling Algorithm

Data: $s[k]$ and $2\lambda\mathbb{Z} \ni \beta_r \geq \|r\|_\infty$.

Result: $\tilde{r}[k] \approx r[k]$.

1) Compute $N = \left\lceil \frac{\log \lambda - \log \beta_r}{\log(T\Omega e)} \right\rceil$.

2) Set $z_{(0)}[k] = (\mathcal{M}_\lambda(\Delta^N s) - \Delta^N s)[k]$.

3) for $n = 0 : N - 2$

(i) $z_{(n+1)}[k] = (\mathcal{S}z_{(n)})[k]$.

(ii) $z_{(n+1)} = 2\lambda \left\lfloor \frac{z_{(n+1)}/\lambda}{2} \right\rfloor$ (rounding to $2\lambda\mathbb{Z}$).

(iii) With $J = 6\beta_r/\lambda$, compute κ_n .

$$\kappa_n = \left\lfloor \frac{\mathcal{S}z_{(n+1)}[1] - \mathcal{S}z_{(n+1)}[J+1]}{12\beta_f} + \frac{1}{2} \right\rfloor$$

(iv) $z_{(n+1)}[k] = z_{(n+1)}[k] + 2\lambda\kappa_n$.

end

4) $\tilde{r}[k] = (\mathcal{S}z_{(N-1)})[k] + s[k] + 2m\lambda, \quad m\mathbb{Z}$.

4.0 EXPERIMENTAL RESULTS

To showcase the potential benefits of the USF for radars, we setup a hardware experiment based on the Coffee Can Radar from MIT³. The prototype setup is shown in Figure 2. This FMCW radar has a carrier frequency of $f_0 = 2.47\text{GHz}$ and a bandwidth of $B = 150\text{MHz}$. The received signal corresponding to a chirp is sampled at 800 points which gives a range resolution of $\delta R = 1\text{m}$ and maximum range recoverable of $R_{max} = 400\text{m}$. The radar is connected to dual-polarised horn antennas [24] and has an acquisition board with 12-bit ADC resolution that spans a range of $\Delta V = 3.3\text{V}$.



Figure 2: Experimental setup.

A snapshot of the real-time processing and data visualisation software⁴ is shown in Figure 3. The experimental setup is shown in Figure 2—two cars driving away from the radar. For all of our plots, the red curves denote conventional ADC data, the green curves denote USF measurements. The signal amplitude is normalized according to the DR of the ADC used for the acquisition, i.e. they lie in $[0, 1]$. The USF measurements are generated in software from the classical measurements. Future work will consider the direct acquisition of signals using US-ADCs developed in [4]. Figure 3 (a) represents the raw signals obtained with classic ADCs and US-ADCs, the threshold of the modulo operator $\mathcal{M}_\lambda(\cdot)$ is set to $\lambda = 0.025$. The radar used in this experiment suffers from a significant RF leakage between the transmit and receive RF chains that completely overshadows the actual received signal from the scene. The signal of interest, coming

³ see <https://spectrum.ieee.org/coffeecan-radar>

⁴ A video of the live acquisition and reconstruction process is available here or <https://www.youtube.com/watch?v=oGzIsncMiTo>

from the reflection of the two moving cars in the scene (see Figure 2), is obtained using a three-pulse canceller Moving Target Indication (MTI) filter [25], i.e.,

$$s_{\text{MTI}}[n] = s^0[n] - 2s^{-1}[n] + s^{-2}[n], \quad (3)$$

where the super-script s^{-i} indicates the index of the reflected signal from every chirp transmission, e.g. $s^0[n]$ is the current reflection and $s^{-2}[n]$ are measurements acquired 2 chirps before. The green curves in Figure 3 (c) has a dynamic range of $\approx \pm 0.01$, which is orders of magnitude below the dynamic of the raw signal in Figure 3(a) that is dominated by the RF leakage. The folded signal in (a) is reconstructed in real-time using the method described in Algorithm 1 and is represented as the green curve in Figure 3(b). As expected, the modulo operation removes the information about the DC component of the signal; the reconstructed signal is centred around zero instead of 0.5. This has no effect in the performance of FMCW radar estimation as the DC component corresponds to a target located at the 0m range bin and is often filtered out.

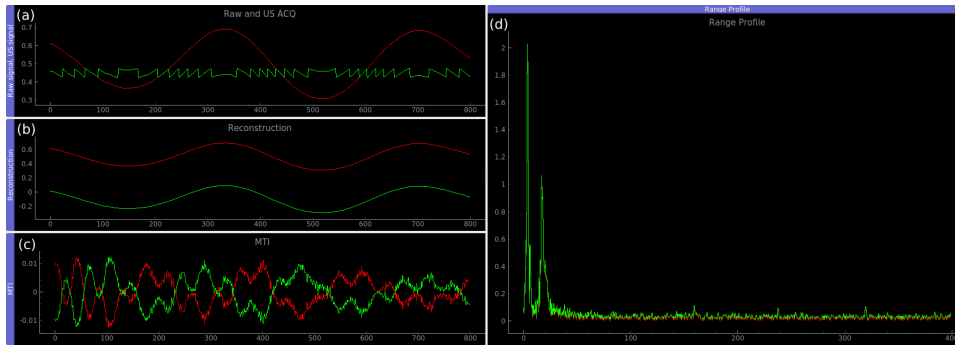


Figure 3: Real-time Python application showcasing the USF for FMCW radar; (a) are the raw signal in red and the corresponding US one in green; (b) is the raw signal in red and the reconstructed signal from US measurements; (c) is the MTI signal obtained using (3) from the classic signal in red and the reconstructed signal in green (the sign of the signal is flipped to aid the visual comparison); (d) is the range profile obtained using FFT from the raw signal in (c) in red and the USF based one in (c) in green.

In Figure 3(c), we compare the application of (3) on both the raw measurements (red) and the reconstruction from modulo measurements (green). The flipped sign is used to ease visual inspection. Because the targets that we are measuring are at small ranges compared to the maximum range R_{max} , the acquired signal is effectively over-sampled and the conditions for perfect reconstruction in Theorem 1 are met; the reconstruction is exact up-to machine precision.

Finally, the range profiles obtained by applying a Fourier transform on the time signals in Figure 3(c) is presented in Figure 3(d). The two range profiles are superimposed as their time signal counterpart are identical.

Table 1: Parameters for radar experiment.

Parameter	Value
Type of Radar	MIT coffee can radar
Operating Frequency	2.47 [GHz]
Bandwidth	150 [MHz]
Sweep Slope	7.5 [MHz/ms]
Number of FFT points	800
Tx and Rx Antennas	1 & 1 Dual Polarised Horn Series DP240
Acquisition	12-bits ADC, $\Delta_V = 3.3V$
Processing	real-time Python script

Remark. It is important to note that, because the US measurements are generated in software from the classic measurements, their resolution in Volts remains the same but their associated number of bits are different. Indeed, the classic ADC can acquire data without saturation in $[0, 1]\Delta V$ with 12-bits of resolution. This corresponds, for the synthesised US-ADC, to a dynamic of $[-0.025, 0.025]\Delta V$ with a dramatically lower resolution of ≈ 7 -bits. Using an actual US-ADC with a resolution that matches its classic counterpart would then increase the absolute resolution and lower the quantization noise, allowing for the USF based processing to outperform the classic acquisition and reconstruction scheme.

5.0 CONCLUSIONS AND FUTURE WORK

Using a hardware setup, in this work we demonstrated for the first time a real-time processing capability for the Unlimited Sampling Framework (USF), on practical FMCW radars. We showed that the USF can be successfully used to acquire and process high dynamic range signals reflected by multiple targets using an FMCW radars. To that end, we developed a real-time demonstrator using the MIT Coffee-Can Radar and showed that the acquisition can be lowered to 5% of the original dynamic range while still providing perfect signal reconstruction with identical range profile. Our preliminary steps raise a number of interesting questions for future work.

- The implementation of the whole chain practically, i.e., using US-ADCs [4] in the pipeline is the next logical step for hardware validation.
- While we considered a simple 1-D range recovery problem, the radar model could be extended to any radar application where the acquired signal is shown to be bandlimited, e.g. Range-Doppler, angle of arrival, MIMO processing.
- This work performed the reconstruction from USF measurements and the range estimation sequentially in order to highlight the fact that HDR signal can be perfectly reconstructed from modulo measurements. One could instead study the recovery of the desired information (e.g. range) directly from the folded measurements.

ACKNOWLEDGEMENT

The authors would like to thank Wallace A. Martins, Ehsan Raei, and Saeid Sedighi for their help in recording radar data. The work of Mohammad Alaei-Kerahroodi and Bhavani Shanakar was supported by FNR CORE SPRINGER Project, ref 12734677. A. Bhandari's work is supported by the UK Research and Innovation council's Future Leaders Fellowship program "Sensing Beyond Barriers" (MRC Fellowship award no. MR/S034897/1).

6.0 REFERENCES

- [1] F. Engels, P. Heidenreich, A. M. Zoubir, F. K. Jondral, and M. Wintermantel, “Advances in automotive radar: A framework on computationally efficient high-resolution frequency estimation,” *IEEE Signal Processing Magazine*, vol. 34, no. 2, pp. 36–46, 2017.
- [2] J. L. Reed, A. D. Lanterman, and J. M. Trostel, “Weather radar: Operation and phenomenology,” *IEEE Aerospace and Electronic Systems Magazine*, vol. 32, no. 7, pp. 46–62, 2017.
- [3] G. Grazzini, M. Pieraccini, F. Parrini, A. Spinetti, G. Macaluso, D. Dei, and C. Atzeni, “An ultra-wideband high-dynamic range gpr for detecting buried people after collapse of buildings,” in *Proceedings of the XIII International Conference on Ground Penetrating Radar*, pp. 1–6, 2010.
- [4] A. Bhandari, F. Krahmer, and T. Poskitt, “Unlimited sampling from theory to practice: Fourier-Prony recovery and prototype ADC,” *IEEE Trans. Sig. Proc.*, Sept. 2021.
- [5] Y. Vanderperren, G. Leus, and W. Dehaene, “An approach for specifying the adc and agc requirements for uwb digital receivers,” in *2006 IET Seminar on Ultra Wideband Systems, Technologies and Applications*, pp. 196–200, 2006.
- [6] P. Smaragdis, “Dynamic range extension using interleaved gains,” *IEEE/ACM Trans. Audio, Speech, Language Process.*, vol. 17, no. 5, pp. 966–973, 2009.
- [7] P. E. Debevec and J. Malik, “Recovering high dynamic range radiance maps from photographs,” in *ACM SIGGRAPH*, ACM Press, 1997.
- [8] A. Bhandari, A. Kadambi, and R. Raskar, *Computational Imaging*. MIT Press, 1st ed., June 2022. open access URL: <https://imagingtext.github.io/>.
- [9] M. Jankiraman, *FMCW Radar Design*. Artech House, 2018.
- [10] J. J. de Witt and W. A. Nel, “Range doppler dynamic range considerations for dechirp on receive radar,” in *2008 Euro. Radar Conf.*, pp. 136–139, 2008.
- [11] Y. Al-Alem, L. Albasha, and H. Mir, “High-resolution on-chip s-band radar system using stretch processing,” *IEEE Sensors Journal*, vol. 16, no. 12, pp. 4749–4759, 2016.
- [12] Z. Tong, R. Renter, and M. Fujimoto, “Fast chirp fmcw radar in automotive applications,” in *IET Intl. Radar Conf.*, pp. 1–4, 2015.
- [13] D. Tang, J. Wang, W. Hu, Z. Peng, Y.-C. Chiang, and C. Li, “A dc-coupled high dynamic range biomedical radar sensor with fast-settling analog dc offset cancelation,” *IEEE Trans. Instrum. Meas.*, vol. 68, no. 5, pp. 1441–1450, 2019.
- [14] K. B. Cooper, S. L. Durden, R. J. Roy, J. V. Siles, R. Rodriguez Monje, R. Dengler, L. Millán, and R. Beauchamp, “Improving fm radar dynamic range using target phase noise cancellation,” *IEEE Journal of Microwaves*, vol. 1, no. 2, pp. 586–592, 2021.
- [15] A. Bhandari, F. Krahmer, and R. Raskar, “On unlimited sampling,” in *Intl. Conf. on Sampling Theory and App. (SampTA)*, July 2017.
- [16] A. Bhandari, F. Krahmer, and R. Raskar, “Unlimited sampling of sparse sinusoidal mixtures,” in *IEEE Intl. Sym. on Information Theory (ISIT)*, June 2018.

- [17] A. Bhandari, F. Kraemer, and R. Raskar, "On unlimited sampling and reconstruction," *IEEE Trans. Sig. Proc.*, vol. 69, pp. 3827–3839, Dec. 2020.
- [18] S. Fernandez-Menduina, F. Kraemer, G. Leus, and A. Bhandari, "DoA estimation via unlimited sensing," in *European Sig. Proc. Conf. (EUSIPCO)*, pp. 1866–1870, Oct. 2020.
- [19] S. Fernandez-Menduina, F. Kraemer, G. Leus, and A. Bhandari, "Computational array signal processing via modulo non-linearities," *IEEE Trans. Sig. Proc.* (in press), July 2021.
- [20] A. Bhandari and F. Kraemer, "HDR imaging from quantization noise," in *IEEE Intl. Conf. on Image Processing (ICIP)*, pp. 101–105, Oct. 2020.
- [21] A. Bhandari, M. Beckmann, and F. Kraemer, "The Modulo Radon Transform and its inversion," in *European Sig. Proc. Conf. (EUSIPCO)*, pp. 770–774, Oct. 2020.
- [22] A. Bhandari, F. Kraemer, and R. Raskar, "Unlimited sampling of sparse sinusoidal mixtures," in *2018 IEEE International Symposium on Information Theory (ISIT)*, pp. 336–340, 2018.
- [23] C. E. Shannon, "Communication in the presence of noise," *Proceedings of the IRE*, vol. 37, no. 1, pp. 10–21, 1949.
- [24] <https://flann.com/products/antennas/dual-polarised-horn-series-dp240/>, 2021. [Online; accessed 21-October-2021].
- [25] M. A. Richards, *Fundamentals of radar signal processing*. McGraw-Hill Education, 2014.